Effects of Cu Feedstock on Intermetallic Compound Formation in Cold Sprayed Cu-Sn Coatings

K. H. Ko[1], H. Lee[2], J. O. Choi*[3]

Department of Materials Science and Engineering, Ajou University, Suwon 443-749, Korea

[1]khko@ajou.ac.kr; [2]materialist@empal.com; *[3]cjo16@lycos.co.kr

Abstract

Cu-Sn composite coatings were deposited using various Cu feedstock powders with different sizes and shapes, and the formation of intermetallic compounds (IMCs) in the coatings was investigated. IMC formation by post-annealing of composite coatings could be affected. In addition, when Cu-Sn composite particles were employed, not only the Cu-Sn composites but also Cu-Sn IMCs (Cu_6Sn_5 and Cu_3Sn) were observed at the interfaces between Cu and Sn particles in the as-sprayed state. In the case of the annealed Cu-Sn coatings, the Cu_6Sn_5 formed in the as-coated coatings was transformed into the Cu_3Sn phase, and the embedded Sn particles were fully changed into the Cu_3Sn phase. However, the intermetallic compound formation of Cu_3Sn was different, depending on the shape and size of the Cu feedstock. Therefore, the deposition of Cu-Sn composite coatings using different Cu particles could have an influence on the formation of IMCs.

Keywords

Cold Spray; Cu-Sn; Composites; Intermetallic; Coatings

Introduction

In the thermal spray process, metallic and ceramic powders are melted by jets emitting hot gas with very high temperatures, after which coatings are formed through the solidification of the melted powders on the substrates. In the cold spray process, however, metallic powders are injected into a de Laval-type nozzle where they are accelerated to high velocities by a supersonic gas stream. When the metallic powders are impinged onto the substrate, their kinetic energy enables the production of coatings with severe deformation. Because the particles are deformed by collision with the substrate, ductile metallic powders must be chosen for the feedstock materials. Also, ceramic powders are unsuitable for feedstock materials in the cold spray process owing to the brittleness. However, in the case of metal (Al)/metal composites coated by the cold spray process, it is very easy to obtain high quality composite coatings because of the deformation behavior. In addition, intermetallic compounds (IMCs) in the coatings are easily obtained by post-annealing, as reported by many researchers. Wang et al. reported the characteristics and influence of heat treatment in Al/Fe composite coatings. Novoselova et al. reported the morphology, porosity, and hardness of Al/Ti composite coatings. Lee et al. investigated the formation of IMCs by post-annealing on cold sprayed Al/Ni and Al/Ti composites. In another case, intermetallic formation was realized by the interaction between the cold sprayed coatings and the substrates. H. Lee et al. reported the Al/Ni interface interaction for intermetallic compound formation produced by cold spraying and post-annealing. H. Bu et al. and K. Spencer et al. investigated the post treatments of Al coating/Mg substrate couples by cold spraying. In the case of Cu/metal composite coatings, few reports were available concerning Cu composite coatings by means of the cold spray process and their IMC formation by means of post-annealing. In this study, Cu-Sn composite coatings were deposited by cold spray on Al substrates, using various types of Cu powders, and annealing studies were carried out to transform the composite coatings into intermetallic compounds. Further, the properties of as-coated and annealed coatings were investigated. The results of these Cu-Sn coatings in the course of the cold spray will be applied in lead-free solders for flip chip connections and the anode electrodes for secondary batteries (Li ion batteries).

Experimental

A home-installed cold spray system was used in this work. The particles were accelerated through a converging–diverging de Laval-type nozzle with a throat diameter of 1 mm (inlet diameter, 7 mm). Pure air, instead of the usual helium and nitrogen, has been

used as both accelerating gas and powder feeding gas. The pressure before entering the gas heater was fixed at 2.0 MPa and the temperature of the gas passing through the nozzle ranged from 200 to 450ºCwhich was measured in the nozzle beside the feedstock feed entrance. The distance between the nozzle and the substrate was 20 mm. The substrate and nozzle were stationary during deposition, and therefore, the deposit was formed in a mountain-like shape. The particle sizes and shapes of as-purchased Sn and Cu were confirmed by scanning electron microscopy (SEM). The Cu-Sn composites were coated onto Al substrates without sand-blasting. The deposition efficiency of the Sn feedstock was higher than that of the Cu feedstock. To produce Cu matrix coatings, a Cu-Sn composite must contain an overwhelming composition of Cu. Therefore, the powder composition ratio of Cu and Sn was 90:10 wt%. The coated samples were annealed at 300ºC under N_2 atmosphere for 6 hours. The annealing heating rate was 5ºC/min and followed by furnace cooling. The structures of the Cu-Sn composite and annealed coatings were analyzed by X-ray powder diffractometry (XRD, Rigaku), and the microstructures and compositions of the coatings were measured by field emission-scanning electron microscopy (FESEM) with energy dispersive spectroscopy (EDS, Philips, XL 30 ESEM-FEG) and optical microscopy (OM).

Results and Discussion

Fig. 1 shows SEM images of the as-purchased Cu and Sn powders used in these experiments. The smaller Cu powders were under 10 μm with spherical shape, while the larger Cu powders were under 44 μm with dendritic shape (Figs. 1(a) and 1(b)). The micro-sized Sn powders were sieved to –325 mesh (≤44 μm) with irregular shape (Fig. 1(c)). Fig. 2 shows XRD patterns of cold sprayed Cu-Sn composite coatings using Cu powders with different shapes and sizes. Peaks corresponding to a newly formed phase were present, suggesting significant chemical interactions among Cu/Sn particles during coating, regardless of the Cu particles' properties. In particular, two types of Cu-Sn intermetallic compounds, Cu_6Sn_5 and Cu_3Sn, without the oxides (SnO, CuO), were observed. In addition, the Cu and Sn feedstock seemed to be neither molten nor semi-molten (Sn melting point: 232ºC) because their flight/coating time was extremely short, so the temperature of the coatings did not reach the melting point of Sn even though the gas temperature was 450ºC. Empirically, when the coatings were exposed to hot gas stream of 450ºC for 10 seconds, the Sn feedstock were melted on the substrate. If the Sn was melted, the coatings would be destroyed (similar to the morphology of thermal sprayed coatings). While coating was made post-annealing, the Cu_6Sn_5 phase disappeared and only Cu_3Sn peaks were observed after complete reaction of the embedded Sn. The Gibbs free energies of the Cu_3Sn and Cu_6Sn_5 phases were negative values, and the Gibb's free energy of the Cu_3Sn phase was lower than that of the Cu_6Sn_5 phase. Fig. 3 shows the OM images of the as-coated Cu-Sn composite coatings by cold spray under different conditions. Similar to the cases of other composite coatings by cold spray, such as Al-metal and Al-ceramic coatings, the "embedded particles phenomena" of Sn particles were observed, accompanied by severe plastic deformation and possible inter-particle bonding between Cu and Sn in the Cu matrix. In spite of the type of the Cu powder and the gas temperature conditions, significant differences in morphology were not observed. Only the plastically deformed and embedded Sn particles (without melting) were found in the Cu matrix despite an increased gas temperature of 450ºC. In addition, it is likely that the embedded soft Sn particles which had high strain energy could interact with the Cu matrix. However, the annealed Cu-Sn composite coatings seemed to differ with respect to Cu powder shape (Fig. 4). It was found that, in the as-coated state, the embedded Sn particles, including the intermetallic compounds (Cu_6Sn_5/Cu_3Sn) reacted with the Cu matrix and grown in the Cu-Sn coatings by using the smaller Cu powders (10 μm). Therefore, the annealed intermetallic compounds (Cu_3Sn) were coarser than the as-coated Sn/IMC particles (Sn/Cu_6Sn_5/Cu_3Sn). Despite the changes in the gas temperature, these results seemed to be the same in all of the annealed Cu-Sn coatings obtained using the smaller Cu powders. It was assumed that the diffusion path of the embedded Sn particles could be provided by the defects resulting from the strain of the smaller Cu (10 μm)-Sn coating systems. In contrast, in the larger Cu (44 μm)-Sn coating systems, the coarsening effect of the embedded Sn particles by post-annealing was less significant than that of the embedded Sn particles in the smaller Cu (10 μm)-Sn coatings. From these results, it was considered that the diffusion route of Sn particles into the Cu matrix or the interaction between Sn and the Cu matrix was very different according to the type of Cu powder.

In order to clearly confirm the compositions and phases of the as-coated and annealed Cu-Sn coatings, coatings prepared under different conditions were measured by the backscattered electron imaging and EDS. Fig. 5 and Fig. 6 show the EDS and backscattered images of the as-coated Cu-Sn coatings, in which the intermetallic compounds were found at the interfaces between Cu and Sn, regardless of gas temperature. Most interestingly, the IMCs of Cu_6Sn_5/Cu_3Sn (confirmed by XRD (Fig. 2)) were formed by the diffusion of Cu particles that were impacted into the Sn particles. Compared to the XRD data, it was also confirmed that the mixed IMCs of Cu-Sn (Cu_6Sn_5/Cu_3Sn) were detected by EDS at the interfaces, and residues of Sn were also observed. Fig. 7 and Fig. 8 show the EDS and backscattered images of the annealed Cu-Sn coatings. The results of the images and EDS were in agreement with the OM and XRD data. To prove that the smaller Cu powders (10 μm) were more severely deformed than the larger Cu powders (44 μm) by the high velocity impact, pure Cu coatings were deposited using both the finer and the coarser powders under the same deposition conditions as the Cu-Sn composite coatings (Fig. 9). As mentioned above, more severe deformation occurred with the smaller Cu particles than that with the larger Cu particles during spraying. As a result of these phenomena, the pores in the Cu coating prepared from the larger Cu powders were easily identified by the lower extent of deformation. Therefore, it was concluded that the more severe deformation as a result of the high velocity of the Cu particles could supply the energy for the coarsening of the IMC (the faster diffusion).

Conclusions

It has been shown that the as-coated and annealed Cu-Sn composites were prepared under different coating conditions (such as the gas temperature and type of Cu powder) on Al substrates by cold spray. In our study of the as-coated Cu-Sn composites, regardless of the type of Cu particles, both raw materials displayed desirable mechanical energy capacities during the high-velocity impact collision coating and could accumulate enough potential energy to overcome the activation barrier of in the course of compounding. Thus, from these results, intermetallic compounds of Cu-Sn in the as-coated state could be obtained at the interfaces between Cu and Sn by high velocity impact. In addition, a greater coarsening of the embedded Sn particles by post-annealing was found for the smaller Cu (10 μm)-Sn composite coatings, which may be due to the higher energy of the smaller Cu particles having the capability to overcome the compounding activation barrier by high velocity impact.

REFERENCES

Bakshi, Srinivasa R., Laha, Tapas, Balani, Kantesh, Agarwal, Arvind, and Karthikeyan, Jeganathan. "Effect of Carrier Gas on Mechanical Properties and Fracture Behaviour of Cold Sprayed Aluminium Coatings." Surface Engineering 23 (2007): 18-22. Accessed January, 2007. doi: 10.1179/174329407X161618.

Bu, Hengyong, Yandouzi, Mohammed, and Jodoin, Bertrand. "Effect of Heat Treatment on the Intermetallic Layer of Cold Sprayed Aluminum Coatings on Magnesium Alloy." Surface and Coatings Technology 205 (2011): 4665-71. Accessed April 3, 2011. doi: 10.1016/j.surfcoat.2011.04.018.

Chidambaram, Vivek, Hald, John, and Hattel, Jesper Henri. "Development of Gold Based Solder Candidates for Flip Chip Assembly." Microelectronics Reliability 49 (2009): 323-30. Accessed December 21, 2008. doi: 10.1016/j.microrel.2008.12.012.

Chiu, TsungChieh, and Lin, KwangLung. "The Difference in the Types of Intermetallic Compound Formed between the Cathode and Anode of a Sn-Ag-Cu Solder Joint under Current Stressing." Intermetallics 17 (2009): 1105-14. Accessed May 26, 2009. doi: 10.1016/j.intermet.2009.05.014.

Cui, WangJun, Wang, Fei, Wang, Jie, Liu, Jaijing, Wang, Congxiao, and Xia, Yongyao. "A Modified Carbothermal Reduction Method for Preparation of High-Performance Nano-Scale Core-Shell Cu_6Sn_5 alloy Anodes in Li-ion Batteries." Journal of Power Sources 196 (2011): 3633-9. Accessed Desember 10, 2010. doi: 10.1016/j.jpowsour.2010.12.025.

Gärtner, Frank. "Advances in Cold Spraying." Surface Engineering 22 (2006): 161-3. Accessed June, 2006. doi: 10.1179/174329406X108906.

Guo, Zhongnan, Hindler, Michael, Yuan, Wenxia, and Mikula, Adolf. "Thermodynamic Properties of Liquid Au-Cu-Sn Alloys Determined from Electromotive Force Measurements." Thermochimica Acta 525 (2011): 183-9. Accessed August 8, 2011. doi: 10.1016/j.tca.2011.08.011.

Islam, M. N., Chan, YanCheong, Rizvi, M. J. and Jillek, Werner. "Investigations of Interfacial Reactions of Sn-Zn based and Sn-Ag-Cu lead-Free Solder Alloys as Replacement for Sn-Pb Solder." Journal of Alloys and Compounds 400 (2005): 136-44. Accessed March 31, 2005. doi: 10.1016/j.jallcom.2005.03.053.

Lee, HaYong, Jung, SeHun, Lee, SooYong, and Ko, KyungHyun. "Fabrication of Cold Sprayed Al-Intermetallic Compounds Coatings by Post Annealing." Materials Science and Engineering A 433 (2006): 139-43. Accessed June 17, 2007. doi: 10.1016/j.msea.2006.06.044.

Lee, HaYong, Lee, SoYong, and Ko, KyungHyun. "Annealing Effects on the Intermetallic Compound Formation of Cold Sprayed Ni, Al Coatings." Journal of Materials Processing Technology 209 (2009): 937-43. Accessed March 2, 2008. doi: 10.1016/.jmatprotec. 2008.03.001.

Lee, HaYong, and Ko, KyungHyun. "Effect of SiC Particle Size on Cold Sprayed Al-SiC Composite Coatings." Surface Engineering 25 (2009): 606-11. Accessed July 2, 2007. doi: 10.1179/174329408X271516.

Lee, HaYong, Lee, SoYong, Shin, HeeJae, and Ko, KyungHyun. "Mechanical Matching and Microstructural Evolution at the Coating/Substrate Interfaces of Cold-Sprayed Ni, Al coatings." Journal of Alloys and Compounds 478 (2009): 636-41. Accessed November 21, 2008. doi: 10.1016/j.jallcom.2008.11.150.

Lee, HaYong, and Ko, KyungHyun. "Fabrication of Porous Al Alloy Coatings by Cold Gas Dynamic Spray Process." Surface Engineering 26 (2010): 395-8. Accessed July 22, 2009. doi: 10.1179/026708409X12490360426124.

Li, Jianfeng, Agyakwa, Pearl A., Johnson, Carole Mark, Zhang, Deen, Hyssain, Tanvir, and McCartney, David Graham. "Characterization and Solderability of Cold Sprayed Sn Cu Coatings on Al and Cu Substrates." Surface and Coatings Technology 204 (2010): 1395-404. Accessed September 9, 2009. doi:10.1016/j.surfcoat. 2009.09.025.

Li, WenYing, Zhang, Chao, Guo, Xyeping, Zhang, Ga, Liao, Hanlin, and Coddet, Christian. "Deposition Characteristics of Al-12Si Alloy Coating Fabricated by Cold Spraying with Relatively Large Powder Particles." Applied Surface Science 253 (2007): 7124-30. Accessed February 2, 2007. doi: 10.1016/j.apsusc.2007.02.142.

Li, WenYing, Zhang, Ga, Liao, Hanlin, and Coddet, Christian. "Characterizations of Cold Sprayed TiN Particle Reinforced Al2319 Composite Coating." Journal of Materials Processing Technology 202 (2008): 508-13. Accessed September 19, 2007. doi: 10.1016/j.jmatprotec. 2007.09.045.

Ma, Xin, Wang, Fengjiang, Qian, Yiyu, and Yoshida, Fusahito. "Development of Cu-Sn Intermetallic Compound at Pb-Free Solder-Cu Joint Interface." Materials Letters 57 (2003): 3361-5. Accessed January 20, 2003. doi: 10.1016/S0167-577X(03)00075-2.

Ning, Xian-Jin, Kim, JinHong, Kim, HyungJun, and Lee, Changhee. "Characteristics and Heat Treatment of Cold-Sprayed Al-Sn Binary Alloy Coatings." Applied Surface Science 255 (2009): 3933-9. Accessed October 10, 2008. doi: 10.1016/j.apsusc.2008.10.074.

Novoselova, Tatiana, Fox, Peter, Morgan, Rhys H., and O'Neill, William "Experimental Study of Titanium/Aluminium Deposits Produced by Cold Gas Dynamic Spray." Surface and Coatings Technology 200 (2006): 2775-83. Accessed October 28, 2004. doi: 10.1016/j.surfcoat.2004.10.133.

Peng, Ming, and Mikula, Adolf. "Thermodynamic Properties of Liquid Cu-Sn-Zn Alloys." Journal of Alloys and Compounds 247 (1997): 185-9. Accessed January, 1997. doi: 10.1016/S0925-8388(96)02575-3.

Spencer, Kevin K., and Zhang, Mingxing. "Heat Treatment of Cold Spray Coatings to Form Protective Intermetallic Layers." Scripta Materialia 61 (2009): 44-7. Accessed March 3, 2009. doi: 10.1016/j.scriptamat. 2009.03.002.

Tao, Yongshan, Xiong, Tianying, Sun, Chao, Jin, Huazi, Du, Hao, and Li, Tiefan. "Effect of α-Al_2O_3 on the Properties of Cold Sprayed Al/α-Al_2O_3 Composite Coatings on AZ91D Magnesium Alloy." Applied Surface Science 256 (2009): 261-6. Accessed August 3, 2009. doi: 10.1016/j.apsusc.2009.08.012.

Villafuerte, Julio C. "Recent Trends in Cold Spray Technology: Looking at the Future." Surface Engineering 26 (2010): 393-4. Accessed August 1, 2010. doi: 10.1179/026708410X12687356948715.

Wang, HongTao, Li, ChangJiu, Yang, GuanJun, and Li, ChengXing. "Cold Spraying of Fe/Al Powder Mixture: Coating Characteristics and Influence of Heat Treatment

on the Phase Structure." Applied Surface Science 255 (2008): 2538-44. Accessed July 22, 2008. doi: 10.1016/j.apsusc.2008.07.127.

Wielage, Bernhard, Podlesak, Harry, Grund, Thomas, and Wank, Andreas, Chemnitz/D. "Cold Gas Sprayed Filler Coatings for Brazing Of Light Alloys." Surface Engineering 115 (2006): 98-102. Accessed April, 2006. doi: 10.1179/174329406X98386.

Wielage, Bernhard, Grund, Thomas, Rupprecht, Christian, and Kuemmel, S. "New Method for Producing Power Electronic Circuit Boards by Cold-Gas Spraying and Investigation of Adhesion Mechanisms." Surface and Coatings Technology 205 (2010): 1115-8. Accessed June 21, 2010. doi: 10.1016/j.surfcoat. 2010.06.020.

Yu, Daquan, Zhao, Zongbin, and Wang, LaiGui. "Improvement on the Microstructure Stability, Mechanical and Wetting Properties of Sn-Ag-Cu Lead-Free Solder with the Addition of Rare Earth Elements." Journal of Alloys and Compounds 376 (2004): 170-5. Accessed January 8, 2004. doi: 10.1016/j.jallcom. 2004.01.012.

Zou, Hefei, Yang, Huajie, and Zhang, Zhefeng. "Coarsening Mechanisms, Texture Evolution and Size Distribution of Cu_6Sn_5 between Cu and Sn-Based Solders." Materials Chemistry and Physics 131 (2011): 190-8. Accessed August 26, 2011. doi: 10.1016 /j.matchemphys. 2011.08.061.

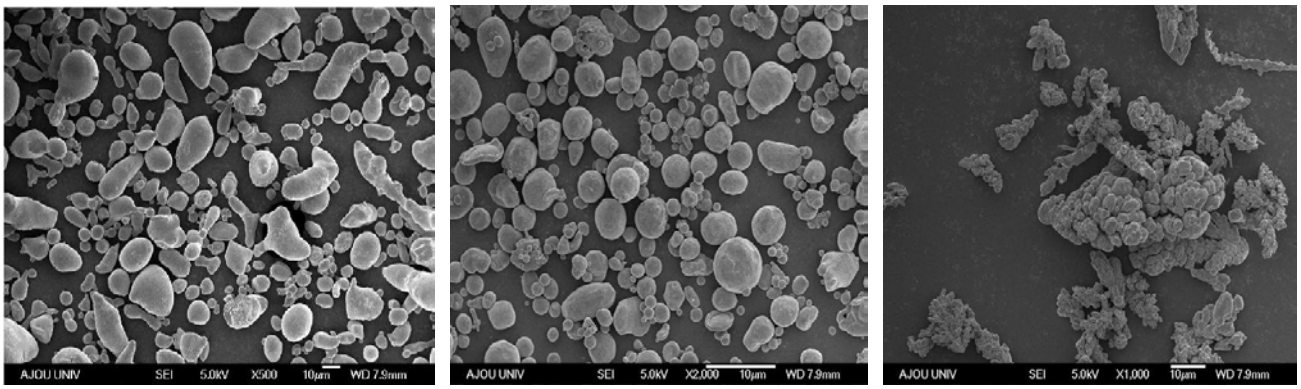

(a) (b) (c)

FIG. 1 SEM IMAGES OF THE AS-PURCHASED CU AND SN POWDERS USED IN THE EXPERIMENT: Cu (10 μm), (b) Cu (44 μm), AND (c) Sn POWDERS (44 μm).

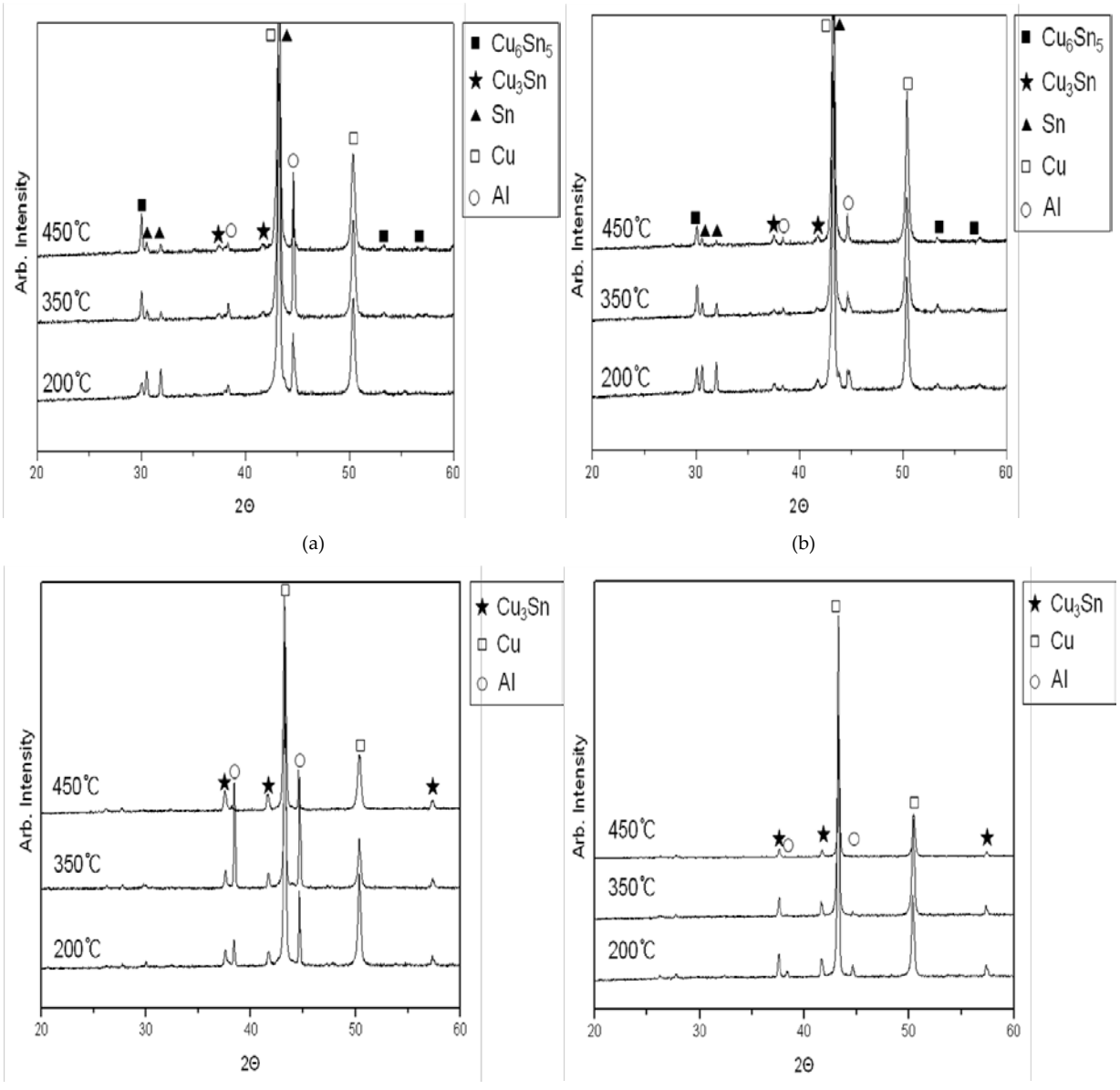

(a) (b)

(c) (d)

FIG. 2 XRD PATTERNS OF CU-SN COMPOSITE COATINGS:

(a) AS-COATED Cu (10 μm)-Sn, (b) AS-COATED Cu (44 μm)-Sn, (c) ANNEALED Cu (10 μm)-Sn, AND (d) ANNEALED Cu (44 μm)-Sn.

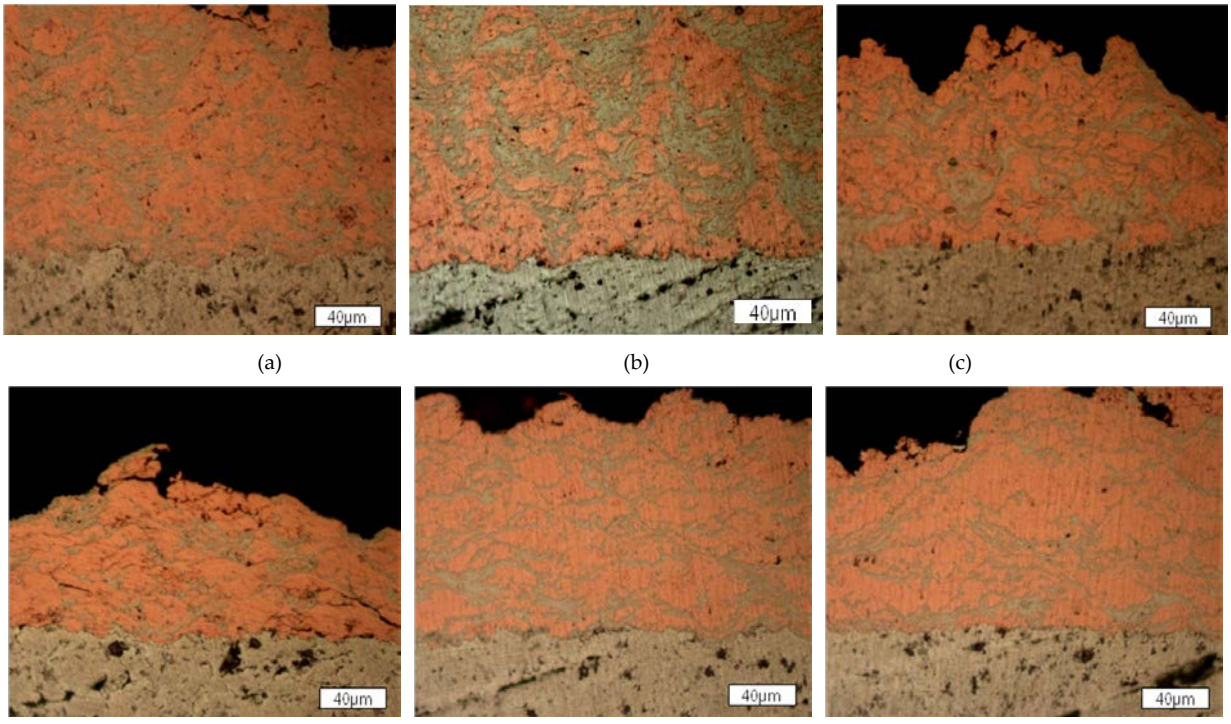

(a) (b) (c)

(d) (e) (f)

FIG. 3 POLISHED CROSS-SECTION IMAGES (OM) OF AS-COATED CU-SN COMPOSITE COATINGS WITH RESPECT TO TYPE OF CU POWDER AND GAS TEMPERATURE CONDITIONS:

(a) Cu (10 µm)-Sn, 200ºC, (b) Cu (10 µm)-Sn, 350ºC, (c) Cu (10 µm)-Sn, 450ºC, (d) Cu (44 µm)-Sn, 200ºC, (e) Cu (44 µm)-Sn, 350ºC, AND (f) Cu (44 µm)-Sn, 450ºC.

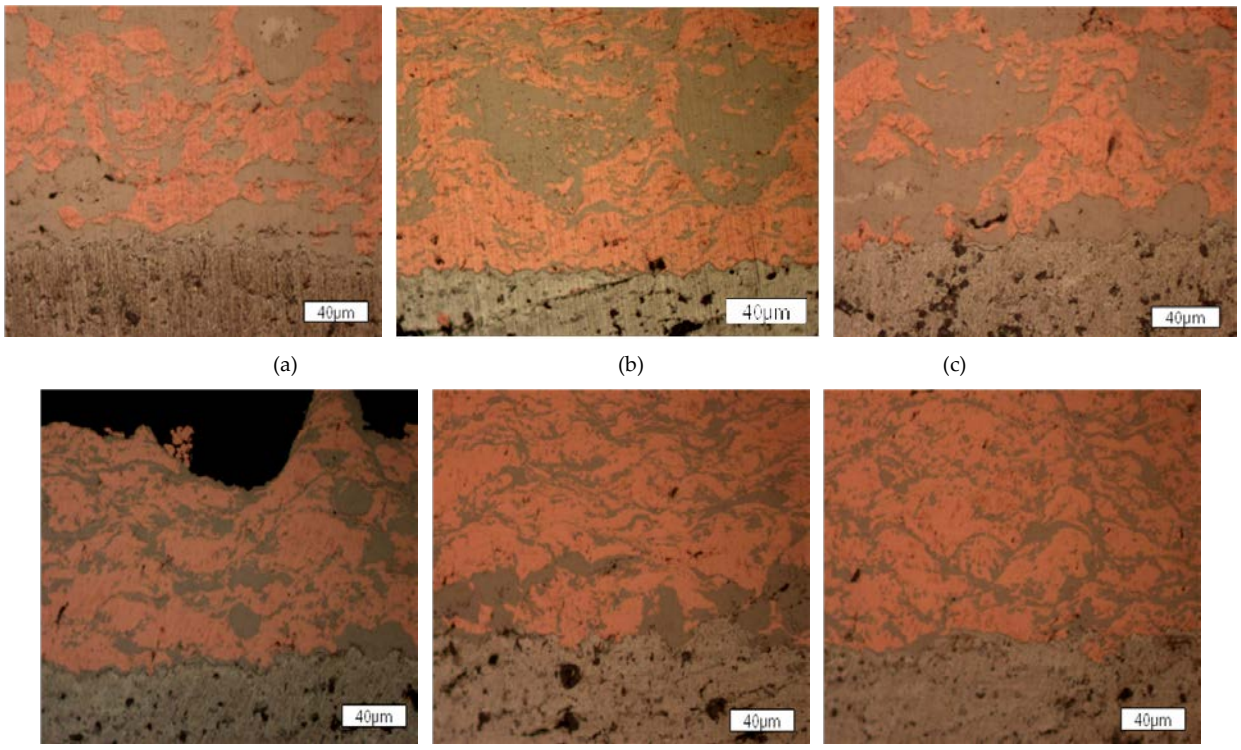

(a) (b) (c)

(d) (e) (f)

FIG. 4 POLISHED CROSS-SECTION IMAGES (OM) OF ANNEALED CU-SN COMPOSITE COATINGS WITH RESPECT TO TYPE OF CU POWDER AND GAS TEMPERATURE CONDITIONS:

(a) Cu (10 µm)-Sn, 200ºC, (b) Cu (10 µm)-Sn, 350ºC, (c) Cu (10 µm)-Sn, 450ºC, (d) Cu (44 µm)-Sn, 200ºC, (e) Cu (44 µm)-Sn, 350ºC, AND (f) Cu (44 µm)-Sn, 450ºC.

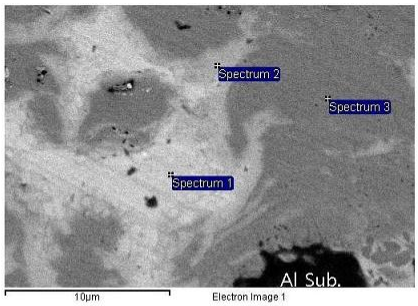

	Sn K (At%)	Cu K (At%)	phase
Spectrum 1	100	0	Sn
Spectrum 2	41.2	58.8	Cu6Sn5+Cu3Sn
Spectrum 3	0	100	Cu

(a)

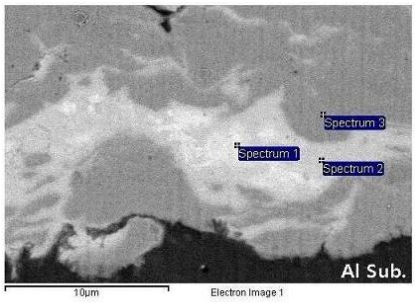

	Sn K (At%)	Cu K (At%)	phase
Spectrum 1	100	0	Sn
Spectrum 2	43.1	56.9	Cu6Sn5+Cu3Sn
Spectrum 3	0	100	Cu

(b)

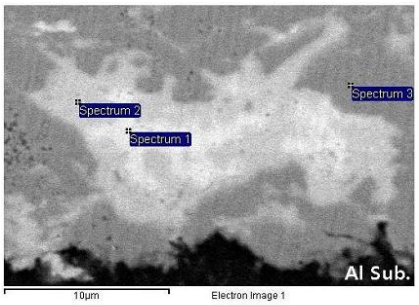

	Sn K (At%)	Cu K (At%)	phase
Spectrum 1	100	0	Sn
Spectrum 2	41.3	58.7	Cu6Sn5+Cu3Sn
Spectrum 3	0	100	Cu

(c)

FIG. 5 THE BACKSCATTERED ELECTRON IMAGES OF AS-COATED CU (10 MM)-SN COMPOSITE COATINGS USING FESEM WITH EDS: AT A GAS TEMPERATURE OF (a) 200ºC, (b) 300ºC, OR (c) 450ºC.

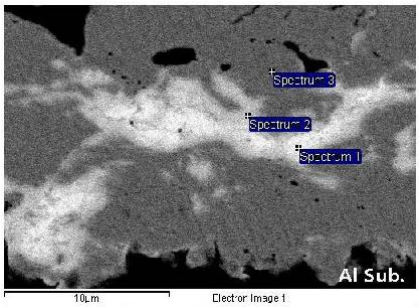

	Sn K (At%)	Cu K (At%)	phase
Spectrum 1	100	0	Sn
Spectrum 2	39.3	60.7	Cu6Sn5+Cu3Sn
Spectrum 3	0	100	Cu

(a)

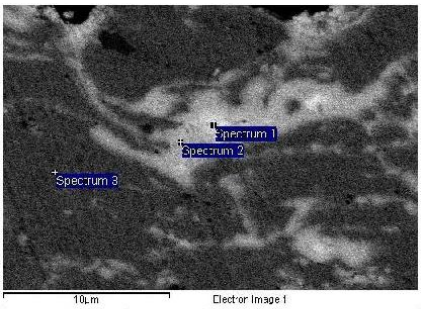

	Sn K (At%)	Cu K (At%)	phase
Spectrum 1	100	0	Sn
Spectrum 2	41.5	58.5	Cu6Sn5+Cu3Sn
Spectrum 3	0	100	Cu

(b)

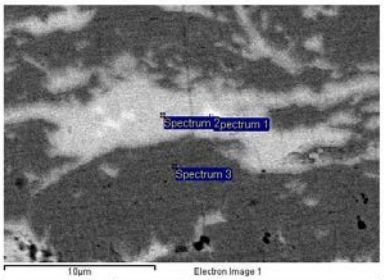

	Sn K (At%)	Cu K (At%)	phase
Spectrum 1	100	0	Sn
Spectrum 2	41.8	58.3	Cu6Sn5+Cu3Sn
Spectrum 3	0	100	Cu

(c)

FIG. 6 THE BACKSCATTERED ELECTRON IMAGES OF AS-COATED CU (44 MM)-SN COMPOSITE COATINGS USING FESEM WITH EDS: AT A GAS TEMPERATURE OF (a) 200ºC, (b) 300ºC, (c) 450ºC.

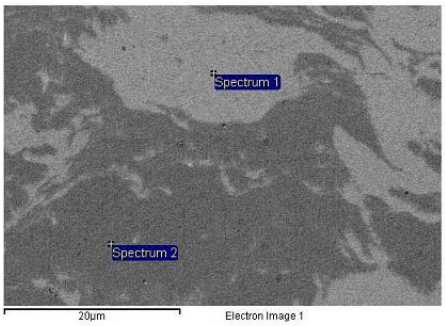

	Sn K (At%)	Cu K (At%)	phase
Spectrum 1	24.6	75.4	Cu3Sn
Spectrum 2	100	0	Cu

(a)

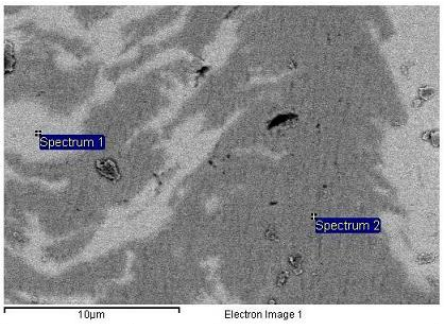

	Sn K (At%)	Cu K (At%)	phase
Spectrum 1	23.4	76.6	Cu3Sn
Spectrum 2	100	0	Cu

(b)

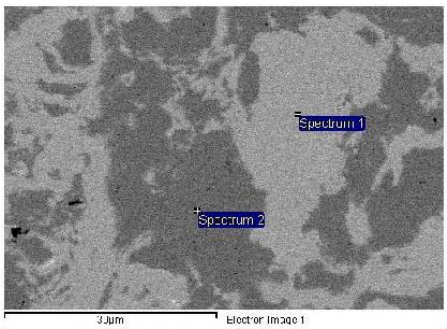

	Sn K (At%)	Cu K (At%)	phase
Spectrum 1	22.5	77.5	Cu3Sn
Spectrum 2	100	0	Cu

(c)

FIG. 7 THE BACKSCATTERED ELECTRON IMAGES OF ANNEALED CU (10 MM)-SN COMPOSITE COATINGS USING FESEM WITH EDS: AT A GAS TEMPERATURE OF (a) 200ºC, (b) 300ºC, OR (c) 450ºC.

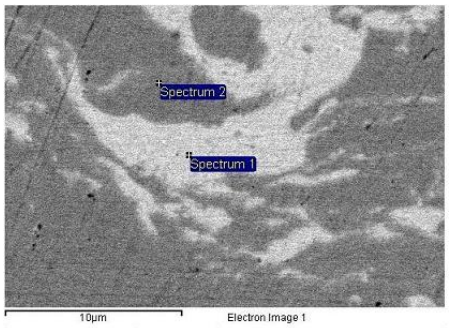

	Sn K (At%)	Cu K (At%)	phase
Spectrum 1	22.9	77.1	Cu3Sn
Spectrum 2	100	0	Cu

(a)

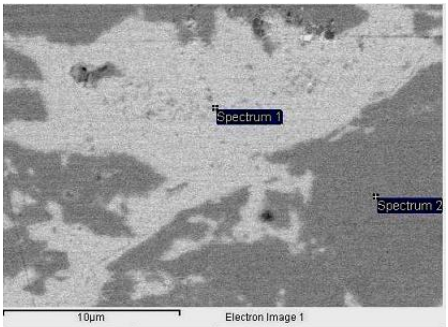

	Sn K (At%)	Cu K (At%)	phase
Spectrum 1	22.2	77.8	Cu3Sn
Spectrum 2	100	0	Cu

(b)

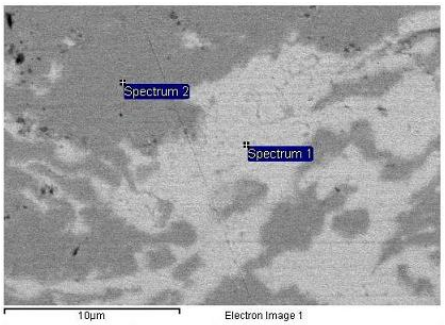

	Sn K (At%)	Cu K (At%)	phase
Spectrum 1	23.4	76.6	Cu3Sn
Spectrum 2	100	0	Cu

(c)

FIG. 8 THE BACKSCATTERED ELECTRON IMAGES OF ANNEALED CU (44 MM)-SN COMPOSITE COATINGS USING FESEM WITH EDS: AT A GAS TEMPERATURE OF (a) 200ºC, (b) 300ºC, OR (c) 450ºC.

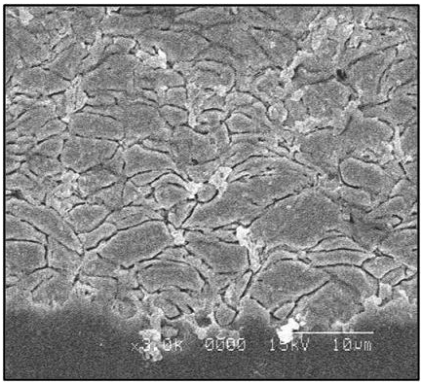

(a)

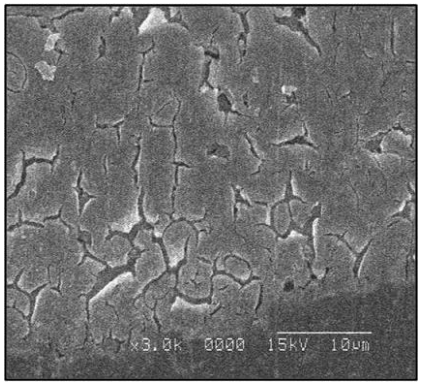

(b)

FIG. 9 CROSS-SECTION IMAGES (SEM) OF PURE CU COATINGS USING DIFFERENT CU POWDERS: (a) 10 μm, (b) 44 μm.